Organic & Biomolecular Chemistry

Cite this: *Org. Biomol. Chem.*, 2011, **9**, 2618

www.rsc.org/obc

COMMUNICATION

Rational design of BINOL-based diimidazolyl ligands: homochiral channel-like mono-component organic frameworks by hydrogen-bond-directed self-assembly†

Li Yang,[b] Fei Yang,[a] Jingbo Lan,[a] Ge Gao,[a] Jingsong You*[a] and Xiaoyu Su*[a]

Received 6th January 2011, Accepted 22nd February 2011
DOI: 10.1039/c1ob00026h

We have developed a synthetic strategy to selectively incorporate the imidazole ring into the 1,1′-bi-2-naphthol (BINOL) skeleton at the different position. The resulting conformationally rigid BINOL-based diimidazolyl ligands bearing both hydrogen-bond-acceptors and -donators can self-assemble into homochiral channel-like mono-component organic frameworks *via* intermolecular O–H···N hydrogen bonds between the phenolic hydroxyl group and the N2 or N4 atom of the imidazole ring.

The creation of supramolecular architectures from organic precursors is currently a highly active area because of aesthetically appealing topologies and potential applications in materials chemistry, host–guest chemistry, and catalysis.[1–3] It is well-known that the construction of such self-assemblies to achieve a proper function of crystalline materials strongly depends on precisely positioning the components within the crystal lattice by means of appropriate noncovalent interactions (*e.g.*, hydrogen bonds, π···π stacking, C–H···π, van der Waals forces and electrostatic interactions, etc.). In particular, the intermolecular hydrogen-bonding interactions are extensively used as a powerful tool in organic self-assemblies owing to their strength and directional properties.[4] Thus, considerable attentions have been devoted to the design of organic assemblies by hydrogen-bond-directed co-crystallizing compounds that have complementary functional groups.[5] As hydrogen-bonding interactions from hydroxyl of carboxylic acid and nitrogen atom have been proved to be an effective organizing force, of particular interest are numerous heterodimers composed of carboxylic acids and basic building blocks such as amines, dipyridines, pyrazines, and their analogues.[6] However, the examples illustrating the phenolic hydroxyl groups as hydrogen-bonding donors are relatively few so far.

1,1′-Binaphthyls have been well-utilized in designing fluorescence sensors, chiral selectors and enantioselective catalysts.[7] On the other hand, imidazole derivatives are ubiquitous in biological and biochemical structure and function, and thus attracted special attention in the construction of metal–organic assemblies in recent years.[8] Following our recent interest in developing organic and organic-metal assemblies with intriguing structures composed of diimidazolyl or tris-monodentate imidazolinyl ligands and dicarboxylic acids or metal ions,[9] we herein wish to incorporate the imidazole moiety into the different positions of 1,1′-bi-2-naphthol (BINOL) to obtain conformationally rigid supramolecular building blocks (*R*)-**1–3** bearing both H-bond-accepting and -donating functionalities. The combination of the imidazole unit with the BINOL skeleton may fulfil the following objectives: firstly, the 2,2′-hydroxyl groups function as hydrogen bond donors.[7b,10] The O–H···N intermolecular hydrogen bonding interactions between the phenolic hydroxyls and the imidazole nitrogen atoms serve as one of main forces to create supramolecular organic frameworks. Secondly, the BINOL skeleton can be functionalized at multi-positions, and the different substituents may dramatically change the dihedral angles, which facilitates the modulation of size, shape, and functionality of self-assemblies.

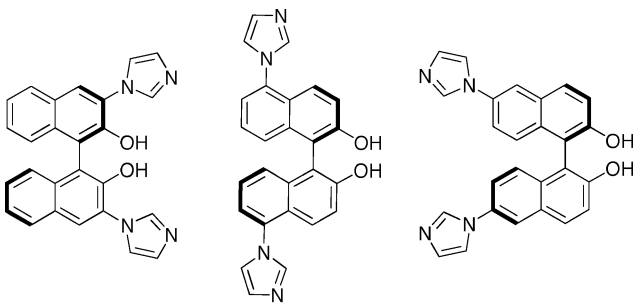

To achieve such supramolecular subunits, the selective modification of the binaphthol skeleton at the different position would be a crucial issue (Scheme 1; for details, see the ESI†). In our synthetic strategy, the readily available (*R*)-BINOL derivatives first went through boration or bromination to obtain the intermediates (*R*)-3,3′-dihydroxyborane-2,2′-dimethoxy-1,1′-dinaphthyl ((*R*)-**6**),[11] (*R*)-5,5′-dibromo-2,2′-diacetoxyl-1,

[a]*Key Laboratory of Green Chemistry and Technology of Ministry of Education, College of Chemistry, Sichuan University, 29 Wangjiang Road, Chengdu, 610064, People's Republic of China. E-mail: jsyou@scu.edu.cn; Fax: +86-28-85412203; Tel: +86-28-85412203*

[b]*State Key Laboratory Cultivation Base for Nonmetal Composites and Functional Materials, National Engineering Technology Center for Insulation Materials, Southwest University of Science and Technology, Mianyang, 621010, People's Republic of China*

† Electronic supplementary information (ESI) available: Experimental procedures, X-ray data collection parameters, X-ray powder diffraction patterns for (*R*)-**1–3**, and copies of ^{1}H and ^{13}C NMR spectra. CCDC reference numbers 806283–806285. For ESI and crystallographic data in CIF or other electronic format see DOI: 10.1039/c1ob00026h

1′-dinaphthyl ((*R*)-**9**), and (*R*)-6,6′-dibromo-2,2′-dimethoxy-methoxy-1,1′-dinaphthyl ((*R*)-**11**),[12] followed by the Cu(I) catalyzed *N*-arylation with imidazole[9b] and removal of the protecting groups to afford the expected ligands (*R*)-**1–3**. Notably, the methods for selective and direct bromination of the binaphthol skeleton at the 5,5′-position are rare hitherto.[13] We surprisingly found that this functionallization could proceed very well at room temperature while the phenolic hydroxyl groups were blocked by the acetyl groups. To our knowledge, it is the first example of the direct bromination at the 5,5′-position in the absence of substituent at the 6,6′-position. We believe that this simple method would open a new way for modifying the backbone of BINOL at the 5,5′-positions.

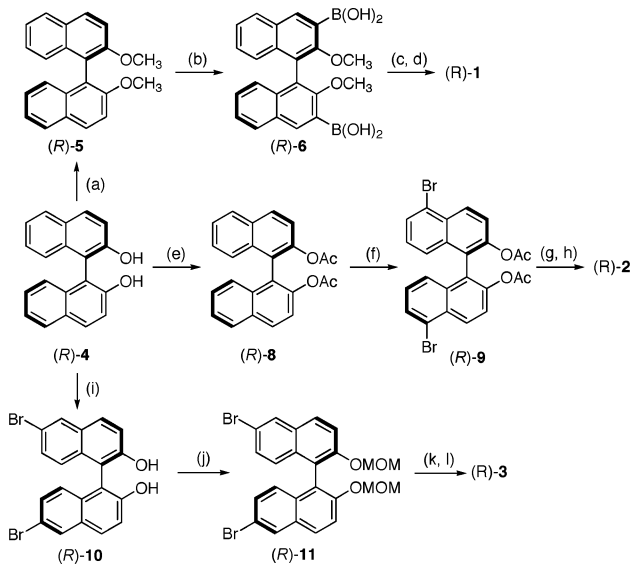

(a) CH_3I, K_2CO_3, acetone, reflux, 95%; (b) *n*BuLi, TMEDA, $B(OCH_3)_3$, Et_2O, -78 °C to rt, 82%; (c) imidazole, CuCl, CH_3OH, air, reflux, 88%; (d) BBr_3, CH_2Cl_2, 0 °C, 85%; (e) Ac_2O, pyridine, CH_2Cl_2, rt, 87%; (f) Br_2, pyridine, CH_2Cl_2, 0 °C to rt, 42%; (g) imidazole, CuI, *N*,*N*-dimethylglycine, K_2CO_3, DMSO, 110 °C; (h) 3M KOH, THF/CH_3OH, reflux, 68% (two steps: g and h); (i) Br_2, CH_2Cl_2, -78 °C, 92%; (j) NaH, MOMCl, THF, 0 °C to rt, 95%; (k) imidazole, CuI, *N*,*N*-dimethylglycine, K_2CO_3, DMSO, 110 °C, 84%; (l) 6M HCl, THF/CH_3OH, reflux, 89%

Scheme 1 Synthetic route of diimidazolyl-substituted BINOLs (*R*)-**1–3**.

With the BINOL-based diimidazolyl building blocks in hand, we investigated the self-assembled architectures of bulk crystalline solids. All crystals suitable for X-ray diffraction analysis were prepared by slow diffusion of 1,4-dioxane into the solutions of (*R*)-**1**, (*R*)-**2** and (*R*)-**3** in dimethylformamide (DMF) at ambient condition, respectively.[14] The structures of three crystals have several common features and distinct differences (see Table S1 for X-ray data collection parameters†). An ORTEP view of (*R*)-**1** is shown in Fig. 1a. As illustrated in Fig. 1b, four molecules of (*R*)-**1** are arranged to form hydrogen-bonded tetramers like a pelton wheel structure stabilized by four intermolecular O–H···N hydrogen bonds between the hydroxyl group and the N2 or N4 atom of imidazolyl moiety. The two type of dihedral angles of the two naphthyl units are around 67° and 77°. Along the crystallographic *b* axis, infinite 2D helical chains are observed (Fig. 1c). Further analysis reveals that each chain is stabilized by hydrogen bonds (2.65 Å, 2.62 Å, and 2.71 Å) and π···π interactions between the imidazole and adjacent parallel naphthol ring (centroid distance 3.696 Å). The two neighboring chains are connected through various van der Waals interactions. More interestingly, the chain aggregates are stacked along the crystallographic *c* axis to create one-dimensional channels (Fig. 1d). The vacant channels are approximately rectangular in cross-section with internal van der Waals dimensions of *ca.* 2.2 × 3.7 Å^2. In (*R*)-**1**, there are not guest molecules in the crystallographic asymmetry unit.

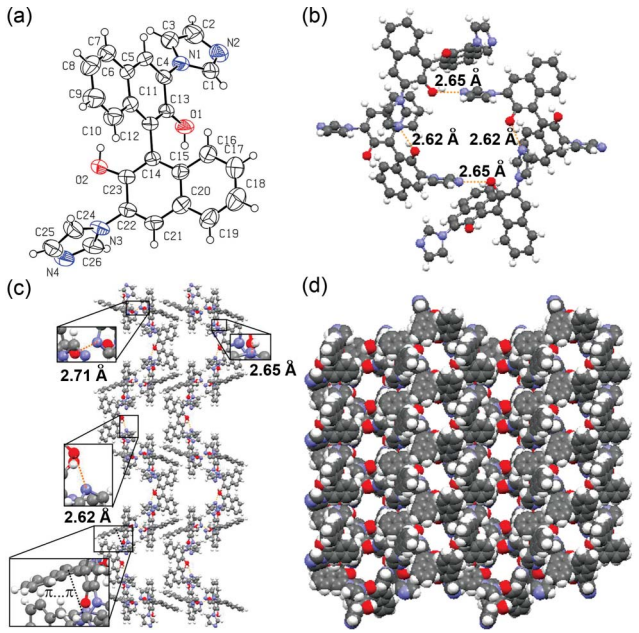

Fig. 1 (a) ORTEP drawing of the molecular structure of (*R*)-**1**. Thermal ellipsoid is set at the 30% probability level. (b) Details of H-bonding interactions of (*R*)-**1** in a typical channel. (c) Infinite 2D helical chains viewed along the *b*-axis. (d) 1-D channel structure viewed along the *c*-axis. Color code: C, dark gray; H, white; N, blue; O, red; Hydrogen bonds, orange dashed line; π···π interaction, black dashed line.

The supramolecular architecture of (*R*)-**2** clearly differs from that of (*R*)-**1**. Ligand (*R*)-**2** does not lead to the formation of hydrogen-bonded tetramers and channel-like structure (Fig. 2). The dihedral angle of the two naphthyl moieties is around 87°. In this arrangement, (*R*)-**2** self-assembles through O–H···N hydrogen bonds (O2···N1 = 2.72 Å, O2–H2···N1 = 158°) to form an infinite 2D helical chain (Fig. 2b), which is further linked by additional intermolecular O–H···N hydrogen bonds (O1···N4 = 2.78 Å, O1–H1···N4 = 164°) to expand to two-dimensional network layers (Fig. 2c). Viewed along the crystallographic *b* axis, the solvent DMF and 1,4-dioxane molecules are independently located in each side of the rhombus network layers in 1 : 1 molar ratio (Fig. S1, ESI†). However, there are not hydrogen bonds between the host and guest molecules.

Similar to (*R*)-**1**, (*R*)-**3** crystallizes in the form of hydrogen-bonded tetramers. As depicted in Fig. 3b, four molecules of (*R*)-**3** are arranged like a square architecture stabilized by four intermolecular O–H···N hydrogen bonds, and the dihedral angles between the two naphthyl units are around 87°. The hydroxyl of BINOL interacts with the imidazolyl nitrogen atom *via* hydrogen bonds (O1···N2 = 2.77 Å, O1–H1···N2 = 130° or O2···N4

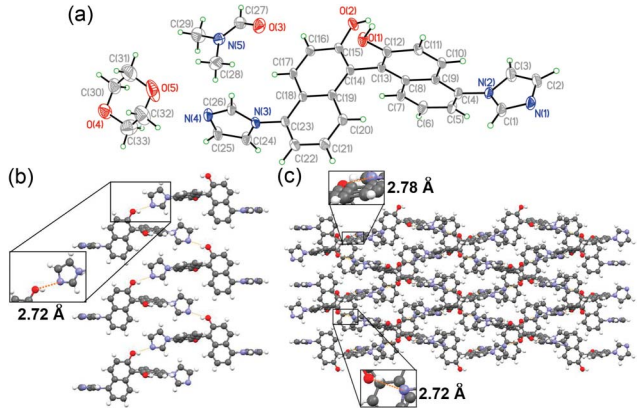

Fig. 2 (a) ORTEP drawing of the molecular structure of (*R*)-**2**. Thermal ellipsoid is set at the 50% probability level. (b) An infinite 2D helical chain viewed along the *b*-axis. (c) 2-D network layer viewed along the *b*-axis. Color code: C, dark gray; N, blue; O, red; H, white; Hydrogen bonds, orange dashed line. In (b) and (c), DMF and 1,4-dioxane solvent molecules were omitted for clarity.

= 2.71 Å, O2–H2···N4 = 172°) to form a single-chain. The two neighboring chains are further connected to form a helical double-chain by weak intermolecular π···π stacking interactions involving between two parallel adjacent imidazole rings (centroid-centroid distance = 3.912 Å) and between two parallel adjacent naphthol rings (centroid-centroid distance = 3.882 Å) (Fig. 3c).

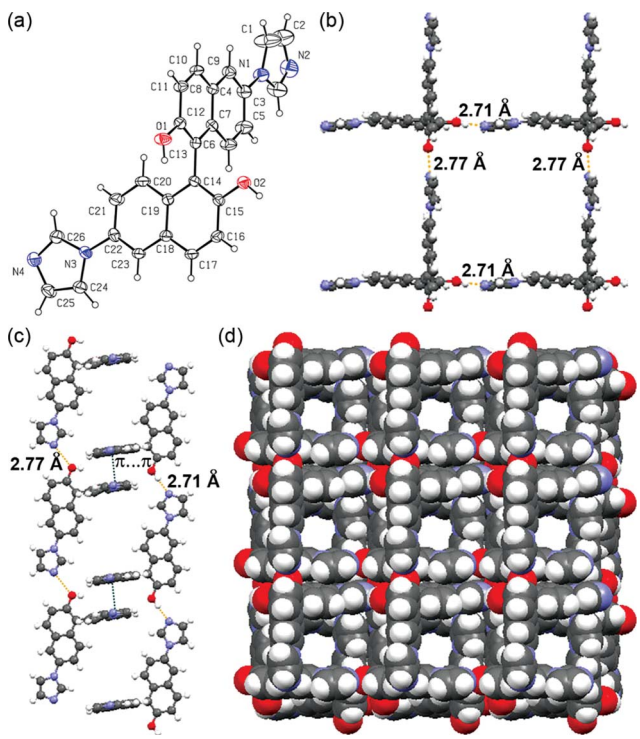

Fig. 3 (a) ORTEP drawing of the molecular structure of (*R*)-**3**. Thermal ellipsoid is set at the 30% probability level. (b) Details of H-bonding interactions of (*R*)-**3** in a typical channel. (c) An infinite 2D helical double-chain viewed along the *b*-axis. (d) 1-D channel structure viewed along the *c*-axis. Color code: C, dark gray; H, white; N, blue; O, red; Hydrogen bonds, orange dashed line; π···π interactions, black dashed line.

Like (*R*)-**1**, the double-chain aggregates pile up along the crystallographic *c* axis to form large 1-D channels (Fig. 3d).

In (*R*)-3, the exact number of guest molecules in the crystallographic asymmetry unit could not be determined according to the Fourier electron densities due to disorder. Considering strong disorganization of the included solvent molecules and the resulting low scattering power of the crystals of (*R*)-**3**, we corrected the observed data by using the SQUEEZE routine in PLATON.[15,16] Omitting guest molecules, the vacant channels are approximately square in cross-section with internal van der Waals dimensions of *ca.* 8.9 × 8.9 Å^2. The solvent accessible volume of (*R*)-**3** calculated using PLATON is 41.1%.[17]

We next examined the structural homogeneity of bulk powder samples of (*R*)-**1–3** by a comparison of experimental and simulated powder XRD (PXRD) patterns. The experimental pattern favorably correlates with the simulated one generated from the single-crystal X-ray diffraction data (Fig. S2–S4, ESI†). The matching of the PXRD's suggests that the bulk powder has a single phase with a similar structure to the single crystals.

In conclusion, we have developed the BINOL-based diimidazolyl supramolecular building blocks ((*R*)-**1–3**) that involve both proton-donating and -accepting sites in the same scaffold. These conformationally rigid subunits can self-assemble into homochiral mono-component organic frameworks from 2-D network layer to channel-like topologies with the modulation of size. The N2 or N4 atom of imidazole ring has been proved to be an excellent hydrogen-bonding acceptor, and can form a strong O–H···N hydrogen bond with the phenolic hydroxyl group, which plays a critical role in the self-assembly. We believe that these BINOL-based diimidazolyl ligands outlined here will find wide applications in various fields of asymmetric bifunctional catalysis and supramolecular self-assembly with organic molecules and metal ions.

Acknowledgements

This work was supported by grants from the National NSF of China (Nos. 20702035, 20972102, 21025205, and 21021001) and PCSIRT0846. We thank the Centre of Testing & Analysis, Sichuan University for PXRD, and NMR measurements.

Notes and references

1 For reviews, see:(*a*) G. R. Desiraju, *Angew. Chem., Int. Ed.*, 2007, **46**, 8342; (*b*) Y. S. Zhao, H. Fu, A. Peng, Y. Ma, D. Xiao and J. Yao, *Adv. Mater.*, 2008, **20**, 2859.

2 For recent examples, see:(*a*) J. Yang, M. B. Dewal, S. Profeta, Jr., M. D. Smith, Y. Li and L. S. Shimizu, *J. Am. Chem. Soc.*, 2008, **130**, 612; (*b*) S. S. Han, H. Furukawa, O. M. Yaghi and W. A. Goddard III, *J. Am. Chem. Soc.*, 2008, **130**, 11580; (*c*) K. J. Msayib, D. Book, P. M. Budd, N. Chaukura, K. D. M. Harris, M. Helliwell, S. Tedds, A. Walton, J. E. Warren, M. Xu and N. B. McKeown, *Angew. Chem., Int. Ed.*, 2009, **48**, 3273; (*d*) J. Tian, P. K. Thallapally, S. J. Dalgarno, P. B. McGrail and J. L. Atwood, *Angew. Chem., Int. Ed.*, 2009, **48**, 5492; (*e*) P. Metrangolo, Y. Carcenac, M. Lahtinen, T. Pilati, K. Rissanen, A. Vij and G. Resnati, *Science*, 2009, **323**, 1461.

3 For selected examples of catalysis, see:(*a*) K. Endo, T. Koike, T. Sawaki, O. Hayashida, H. Masuda and Y. Aoyama, *J. Am. Chem. Soc.*, 1997, **119**, 4117; (*b*) Y. Zhang, S. N. Riduan and J. Y. Ying, *Chem.–Eur. J.*, 2009, **15**, 1077.

4 (*a*) C. B. Aakeröy and K. R. Seddon, *Chem. Soc. Rev.*, 1993, **22**, 397; (*b*) J. W. Steed and J. L. Atwood, *Supramolecular Chemistry*, John Wiley & Sons, Ltd.: Chichester, 2000.

5 For selected examples, see:(*a*) V. R. Pedireddi, S. Chatterjee, A. Ranganathan and C. N. R. Rao, *J. Am. Chem. Soc.*, 1997, **119**, 10867; (*b*) C. B. Aakeröy, A. M. Beatty and B. A. Helfrich, *J. Am. Chem. Soc.*, 2002, **124**, 14425; (*c*) I. Boldog, E. B. Rusanov, J. Sieler, S. Blaurock and K. V. Domasevitch, *Chem. Commun.*, 2003, 740; (*d*) K. E. Maly, E. Gagnon, T. Maris and J. D. Wuest, *J. Am. Chem. Soc.*, 2007, **129**, 4306.
6 For selected examples, see:(*a*) C. B. Aakeröy, A. M. Beatty and B. A. Helfrich, *Angew. Chem., Int. Ed.*, 2001, **40**, 3240; (*b*) A. Ballabh, D. R. Trivedi and P. Dastidar, *Cryst. Growth Des.*, 2005, **5**, 1545; (*c*) B. R. Bhogala, S. Basavoju and A. Nangia, *Cryst. Growth Des.*, 2005, **5**, 1683; (*d*) T. R. Shattock, P. Vishweshwar, Z. Wang and M. J. Zaworotko, *Cryst. Growth Des.*, 2005, **5**, 2046; (*e*) M. Sarkar and K. Biradha, *Cryst. Growth Des.*, 2006, **6**, 202; (*f*) D. R. Trivedi and P. Dastidar, *Cryst. Growth Des.*, 2006, **6**, 1022; (*g*) Y. Imai, K. Kawaguchi, K. Murata, T. Sato, R. Kuroda and Y. Matsubara, *Org. Lett.*, 2008, **10**, 469; (*h*) Y. Imai, K. Murata, T. Sato, R. Kuroda and Y. Matsubara, *Org. Lett.*, 2008, **10**, 3821; (*i*) A. Delori, E. Suresh and V. R. Pedireddi, *Chem.–Eur. J.*, 2008, **14**, 6967; (*j*) Y.-B. Men, J. Sun, Z.-T. Huang and Q.-Y. Zheng, *Angew. Chem., Int. Ed.*, 2009, **48**, 2873.
7 For reviews, see:(*a*) Y. Chen, S. Yekta and A. K. Yudin, *Chem. Rev.*, 2003, **103**, 3155; (*b*) L. Pu, *Chem. Rev.*, 2004, **104**, 1687.
8 For selected recent examples, see:(*a*) L. Dobrzańska, G. O. Lloyd, H. G. Raubenheimer and L. J. Barbour, *J. Am. Chem. Soc.*, 2005, **127**, 13134; (*b*) L. Dobrzańska, G. O. Lloyd, H. G. Raubenheimer and L. J. Barbour, *J. Am. Chem. Soc.*, 2006, **128**, 698; (*c*) I. Imaz, D. Maspoch, C. Rodríguez-Blanco, J. M. Pérez-Falcón, J. Campo and D. Ruiz-Molina, *Angew. Chem., Int. Ed.*, 2008, **47**, 1857; (*d*) R. Nishiyabu, N. Hashimoto, T. Cho, K. Watanabe, T. Yasunaga, A. Endo, K. Kaneko, T. Niidome, M. Murata, C. Adachi, Y. Katayama, M. Hashizume and N. Kimizuka, *J. Am. Chem. Soc.*, 2009, **131**, 2151; (*e*) R. Nishiyabu, C. Aimé, R. Gondo, T. Noguchi and N. Kimizuka, *Angew. Chem., Int. Ed.*, 2009, **48**, 9465.
9 (*a*) W.-H. Wang, P.-H. Xi, X.-Y. Su, J.-B. Lan, Z.-H. Mao, J.-S. You and R.-G. Xie, *Cryst. Growth Des.*, 2007, **7**, 741; (*b*) F. Yang, S. Wei, C.-A. Chen, P. Xi, L. Yang, J. Lan, H.-M. Gau and J. You, *Chem.–Eur. J.*, 2008, **14**, 2223; (*c*) L. Yan, Z. Wang, M.-T. Chen, N. Wu, J. Lan, X. Gao, J. You, H.-M. Gau and C.-T. Chen, *Chem.–Eur. J.*, 2008, **14**, 11601; (*d*) S. Zhang, S. Yang, J. Lan, S. Yang and J. You, *Chem. Commun.*, 2008, 6170; (*e*) S. Zhang, S. Yang, J. Lan, Y. Tang, Y. Xue and J. You, *J. Am. Chem. Soc.*, 2009, **131**, 1689; (*f*) L. Yan, Y. Xue, G. Gao, J. Lan, F. Yang, X. Su and J. You, *Chem.–Eur. J.*, 2010, **16**, 2250.
10 T. Shimasaki, S.-I. Kato, K. Ideta, K. Goto and T. Shinmyozu, *J. Org. Chem.*, 2007, **72**, 1073.
11 Q.-S. Lu, L. Dong, J. Zhang, J. Li, L. Jiang, Y. Huang, S. Qin, C.-W. Hu and X.-Q. Yu, *Org. Lett.*, 2009, **11**, 669.
12 M.-H. Xu, J. Lin, Q.-S. Hu and L. Pu, *J. Am. Chem. Soc.*, 2002, **124**, 14239.
13 (*a*) D. J. Cram, R. C. Helgeson, S. C. Peacock, L. J. Kaplan, L. A. Domeier, P. Moreau, K. Koga, J. M. Mayer, Y. Chao, M. G. Siegel, D. H. Hoffman and G. D. Y. Sogah, *J. Org. Chem.*, 1978, **43**, 1930; (*b*) S. Zhang, Y. Liu, H. Huang, L. Zheng, L. Wu and Y. Cheng, *Synlett*, 2008, **6**, 853.
14 The crystal parameters, data collection and refinement results for CCDC-806283 ((*R*)-**1**), CCDC-806284 ((*R*)-**2**), and CCDC-806285 ((*R*)-**3**) are summarized in Supporting Information (Table S1, ESI†). These data can also be obtained free of charge from the Cambridge Crystallographic Data Centre *via* www.ccdc.cam.ac.uk/data_request/cif.
15 The crystallographic data for (*R*)-**3** with the guest molecules squeezed are given in Table S1 (ESI†).
16 (*a*) A. L. Spek, *Acta Crystallogr., Sect. D: Biol. Crystallogr.*, 2009, **65**, 148; (*b*) M. Mastalerz, M. W. Schneider, I. M. Oppel and O. Presly, *Angew. Chem., Int. Ed.*, 2011, **50**, 1046; (*c*) M. Xue and C.-F. Chen, *Chem. Commun.*, 2011, **47**, 2318.
17 A. L. Spek, *PLATON, A Multipurpose Crystallographic Tool*, Utrecht University: Utrecht, The Netherlands, 2001.